

UC Irvine

UC Irvine Previously Published Works

Title

Retinal pigmented epithelial cells obtained from human induced pluripotent stem cells possess functional visual cycle enzymes in vitro and in vivo.

Permalink

<https://escholarship.org/uc/item/9hh2j0t1>

Journal

Journal of Biological Chemistry, 288(48)

Authors

Maeda, Tadao

Lee, Mee

Palczewska, Grazyna

et al.

Publication Date

2013-11-29

DOI

10.1074/jbc.M113.518571

Peer reviewed

Retinal Pigmented Epithelial Cells Obtained from Human Induced Pluripotent Stem Cells Possess Functional Visual Cycle Enzymes *in Vitro* and *in Vivo**

Received for publication, September 12, 2013, and in revised form, October 14, 2013. Published, JBC Papers in Press, October 15, 2013, DOI 10.1074/jbc.M113.518571

Tadao Maeda^{†§1}, Mee Jee Lee[‡], Grazyna Palczewska[¶], Stefania Marsili[‡], Paul J. Tesar^{||}, Krzysztof Palczewski[§], Masayo Takahashi^{**}, and Akiko Maeda^{†§2}

From the Departments of [†]Ophthalmology and Visual Sciences, [§]Pharmacology, and ^{||}Genetics, Case Western Reserve University, Cleveland, Ohio 44106, [¶]Polgenix, Inc., Cleveland, Ohio 44106, and the ^{**}Laboratory for Retinal Regeneration, Center for Developmental Biology, RIKEN, Kobe 650-0047, Japan

Background: The visual (retinoid) cycle activity in human iPS-derived RPE (hiPS-RPE) cells has not been fully examined.

Results: hiPS-RPE cells showed a functional visual cycle in both *in vitro* and *in vivo*.

Conclusion: hiPS-RPE cell could provide potential treatment options for retinal degenerative diseases.

Significance: hiPS-RPE cells with functional visual cycle proteins potentially could remedy certain degenerative retinal diseases.

Differentiated retinal pigmented epithelial (RPE) cells have been obtained from human induced pluripotent stem (hiPS) cells. However, the visual (retinoid) cycle in hiPS-RPE cells has not been adequately examined. Here we determined the expression of functional visual cycle enzymes in hiPS-RPE cells compared with that of isolated wild-type mouse primary RPE (mpRPE) cells *in vitro* and *in vivo*. hiPS-RPE cells appeared morphologically similar to mpRPE cells. Notably, expression of certain visual cycle proteins was maintained during cell culture of hiPS-RPE cells, whereas expression of these same molecules rapidly decreased in mpRPE cells. Production of the visual chromophore, 11-*cis*-retinal, and retinosome formation also were documented in hiPS-RPE cells *in vitro*. When mpRPE cells with luciferase activity were transplanted into the subretinal space of mice, bioluminescence intensity was preserved for >3 months. Additionally, transplantation of mpRPE into blind *Lrat*^{-/-} and *Rpe65*^{-/-} mice resulted in the recovery of visual function, including increased electrographic signaling and endogenous 11-*cis*-retinal production. Finally, when hiPS-RPE cells were transplanted into the subretinal space of *Lrat*^{-/-} and *Rpe65*^{-/-} mice, their vision improved as well. Moreover, histological analyses of these eyes displayed replacement of dysfunctional RPE cells by hiPS-RPE cells. Together, our results show that hiPS-RPE cells can exhibit a functional visual cycle *in vitro* and *in vivo*. These cells could provide potential treatment options for certain blinding retinal degenerative diseases.

The retinal pigmented epithelium (RPE)³ is a monolayer of cells, located in the rear of the eye between Bruch's membrane and the neural retina which plays an essential role in maintaining photoreceptor function and survival. Thus, dysfunction or death of RPE cells can cause various human retinal degenerative diseases such as retinitis pigmentosa, congenital progressive retinal dystrophies, and age-related macular degeneration (AMD), one of the leading causes of legal blindness in industrialized countries (1–3). The limited benefits of current medical and surgical interventions for these diseases accentuate the need to establish more effective therapies including the development of a cell-based transplantation strategy. Various cell types have been tested for use in RPE cell replacement including immortalized cell lines (4), primary RPE cells from adult and fetal tissues (5), and RPE differentiated from human embryonic stem (ES) cells (6). Recently, induced pluripotent stem (iPS) cells have been established as an alternative cell source for transplantation (6). iPS cells are morphologically identical to ES cells, which display similar gene expression profiles and epigenetic status and have the potential to form any type of cell within the body. iPS cells have been employed to generate several types of differentiated cells for future treatment options and study tools in various diseases, such as diabetes, cardiovascular diseases, Parkinson disease and AMD (7).

Several research groups have reported that human ES and iPS cells can be differentiated into RPE cells which display some degree of RPE functionality, including phagocytosis and growth factor secretion (8, 9). However, the visual (retinoid) cycle in hiPS-derived RPE (hiPS-RPE) cells has not been rigorously

* This work was supported, in whole or in part, by National Institutes of Health Grants K08EY019031, K08EY019880, R01EY022658, R01EY009339, R24EY021126, R44AG043645, and P30EY011373. This work was also supported by the Research to Prevent Blindness Foundation, the Foundation Fighting Blindness, the Midwest Eye Banks, and the Ohio Lions Eye Research Foundation.

¹ To whom correspondence may be addressed: Case Western Reserve University, 10900 Euclid Ave., Cleveland, OH 44106, USA. Tel.: 216-368-6103; Fax: 216-368-3171; E-mail: txm88@case.edu.

² To whom correspondence may be addressed: Case Western Reserve University, 10900 Euclid Ave., Cleveland, OH 44106. Tel.: 216-368-0670; Fax: 216-368-3171; E-mail: aam19@case.edu.

³ The abbreviations used are: RPE, retinal pigmented epithelium; AMD, age-related macular degeneration; BLI, bioluminescence imaging; CRALBP, cellular retinaldehyde-binding protein; ERG, electroretinogram; hiPS, human induced pluripotent stem; iPS, induced pluripotent stem; LCA, Leber congenital amaurosis; LRAT, lecithin:retinol acyltransferase; Luc, luciferase; mpRPE, mouse primary retinal pigmented epithelium; Pn, passage number; qRT-PCR, quantitative RT-PCR; RDH, retinol dehydrogenase; RLBP, retinaldehyde-binding protein; RPE65, retinal pigment epithelium-specific 65-kDa protein; SD-OCT, spectral domain optical coherence tomography; STRA6, stimulated by retinoic acid gene 6; TEM, transmission electron microscope; TPM, two-photon microscopy.

examined. The visual cycle consists of a series of enzymatic reactions occurring in both photoreceptor outer segments and RPE cells. The function of this cycle is to regenerate photoreceptor visual pigments continuously by supplying the visual chromophore, 11-*cis*-retinal, and to remove potentially toxic retinoid byproducts generated by photoreceptor cells upon photon absorption. Therefore, this cycle is indispensable to maintain vision and the health of the retina. It is well recognized that many biochemical reactions in this cycle occur in the RPE (10, 11). Among them, two enzymes, retinal pigment epithelium-specific 65-kDa protein (RPE65) and lecithin:retinol acyltransferase (LRAT) are essential components. Abnormal function of either enzyme results in a severe congenital retinal degeneration called Leber congenital amaurosis (LCA) (12, 13).

Despite the potential of iPS-RPE cells for the future therapeutic applications, it is still not known whether or not they have a functional visual cycle. Moreover, even if they do, the question remains as to whether these cells can restore visual function in degenerative retinal diseases resulting from a dysfunctional visual cycle.

In this study, the expression of molecules involved in the visual cycle in RPE cells was examined in both hiPS-RPE and mouse primary RPE (mpRPE) cells. Production of the visual chromophore, 11-*cis*-retinal, was also assessed in cultured cells. Furthermore, visual cycle function was evaluated following transplantation of both types of cells into the subretinal space of blind *Lrat*^{-/-} and *Rpe65*^{-/-} mice. This study demonstrates that hiPS-RPE cells can maintain a functional visual cycle thus providing a novel therapeutic option for retinal degenerative diseases such as retinitis pigmentosa and AMD associated with RPE damage.

EXPERIMENTAL PROCEDURES

Mice—*Lrat*^{-/-} mice were bred as previously described (14), and *Rpe65*^{-/-} mice were originally generated by Dr. T. M. Redmond (NEI, National Institutes of Health) (15). FVB-Tg (CAG-Luc, GFP), C57BL/6J, and C57BL/6J-*Tyr*^{c-2J}/J mice were purchased from the Jackson Laboratory. Systemic luciferase-expressing mice were bred by crossing C57BL/6J with FVB-Tg (CAG-Luc, GFP) mice. All mice were genotyped by established methods provided by the Jackson Laboratory. Mice were housed in the animal facility at the School of Medicine, Case Western Reserve University, where they were maintained either in the dark or under a 12-h light (~10 lux)/12-h dark cycle. Manipulations in the dark were conducted under dim red light transmitted through a Kodak number 1 safelight filter (transmittance >560 nm). All animal procedures and experiments were approved by the Case Western Reserve University Institutional Animal Care and Use Committees (IACUC) and conformed to recommendations of both the American Veterinary Medical Association Panel on Euthanasia and the Association of Research for Vision and Ophthalmology.

Isolation of Primary RPE Cells—RPE cells were isolated from eyes of 10- to 12-day-old mice as described previously (16). Briefly, enucleated eyes were incubated in 2% dispase (Invitrogen) solution for 45 min in a 37 °C water bath with gentle decanting every 15 min. After removal of the neural retina, sheets of RPE were peeled away from the choroid and pipetted

into a tube containing DMEM plus streptomycin/penicillin and 10% fetal bovine serum.

Differentiation of iPS Cells into RPE Cells—hiPS cells (HiPS-RIKEN-1A derived from human umbilical cord, P29–P30) and CWRU22 cells derived from human fibroblasts, P22–23) were purchased from RIKEN Bioresource Center (Tsukuba, Japan) or obtained from the Pluripotent Stem Cell Facility, Case Western Reserve University. These cell lines were established in accordance with the tenets of The Declaration of Helsinki. hiPS cell lines were maintained in Primate ES Cell Medium (ReproCell, Yokohama, Japan) and radiated mouse embryonic fibroblast feeder. Differentiation of hiPS cells to RPE cells was performed as detailed previously (17). Briefly, hiPS clumps were moved to a nonadhesive 2-methacryloyloxyethyl phosphorylcholine-treated dish (Nunc, Rochester, NY) in maintenance medium for 3 days with SB-431542 (Invitrogen) and CKI-7 (Sigma-Aldrich) and then in differentiation medium for 21 days with KSR (Invitrogen) (20–10%). On day 21, cells were plated onto poly-D-lysine/laminin/fibronectin-coated eight-well culture slides (BD Biocoat; BD Biosciences) at a density of 15–20 aggregates/cm². Cells were cultured in 10% KSR-containing differentiation medium until day 60. After differentiation, hiPS-RPE cell was maintained in RPE maintenance medium (18).

RT-PCR and Quantitative RT-PCR (qRT-PCR)—Total RNA was isolated with a RNeasy Mini kit (Qiagen), and cDNA was synthesized from 200 ng of total RNA by using SuperScriptTM II Reserve Transcriptase (Invitrogen) and following the manufacturer's instructions. Real-time PCR amplification was performed with iQTM SYBR[®] Green Supermix (Bio-Rad) with Eppendorf Mastercycler ep realplex. Primer sequences for mice were: *Rpe65*-H1 forward, 5'-tcattgtcacagcaggattc-3' and reverse, 5'-aaagcacaggtgccaattc-3'; *Lrat*-H1 forward, 5'-cagggaccattttatccac-3' and reverse, 5'-agccaccttgcaatgactc-3'; *Rdh5*-H1 forward, 5'-cctctggagcagaagacctg-3' and reverse, 5'-ctgtgttagcctatggtgtg-3'; *Strat6*-H3 forward, 5'-gccagtcacatccaggagtc-3' and reverse, 5'-agcaactgcatcctcttctc-3'; *Rlbp1*-H1 forward, 5'-aggagctgtacaggcacag-3' and reverse, 5'-gaggcgaagttcacatagc-3'; *Gapdh*-Y1 forward, 5'-gtgttctaccctcaatgtg-3' and reverse, 5'-aggagacaacctggtctca-3'. Primer sequences for humans were the following: *H-RPE65*-H2 forward, 5'-accagtgagggaagattac-3' and reverse, 5'-ttcctgtctgtctgctgagc-3'; *H-LRAT*-H1 forward, 5'-acctgacctactggatc-3' and reverse, 5'-acaataacgcccaggatgag-3'; *H-RDH5*-H1 forward, 5'-cctgtgaccaacctggagag-3' and reverse, 5'-ggttaggtccgggtcacag-3'; *H-STRA6*-H1 forward, 5'-acctccacagccaggatc-3' and reverse, 5'-gccagcaggtaggagacatc-3'; *H-RLBP1*-H2 forward, 5'-ggagaagctgctggagaatg-3' and reverse, 5'-agaaggcttgaccattg-3'; *H-GAPDH*-H2 forward, 5'-caatgacctctcattgacc-3' and reverse, 5'-gacaagctcccgttctcag-3'. Relative expression levels of genes were normalized by GAPDH.

Immunoblotting—SDS-PAGE was performed with 12.5% polyacrylamide gels, and proteins were electrophoretically transferred onto Immobilon-P (Millipore). The membrane was blocked with 3% BSA in 10 mM phosphate buffer, pH 7.5, containing 100 mM NaCl, and incubated for 3–16 h with primary antibody. A secondary antibody conjugated with alkaline phosphatase (Promega) was used at a dilution of 1:5,000. Ab binding

Transplantation of Functional RPE Rescues Vision in Mice

was detected after incubation with nitro blue tetrazolium/5-bromo-4-chloro-3-indolyl phosphate (Promega). Anti-RPE65 antibody was generated as before (19). Anti- β -actin antibody was purchased from Novus Biologicals (Littleton, CO), and anti- β -tubulin antibody was obtained from DSHA at the University of Iowa.

Isomerization Assay and Retinoid Analysis—RPE cells at 3×10^4 cells/well were seeded into 48-well plates, and one retina obtained from a *Lrat*^{-/-} mouse was added to each well in the presence of 30 μ M recombinant CRALBP. To initiate isomerization, 10 μ M all-*trans*-retinol was mixed into the well, and plates were incubated at 37 °C for 16 h in the dark. Retinoid analyses were carried out on retinas after incubation by using a HPLC method published previously (20). Quantification of retinoids in the eyes was performed with two eyes by the same HPLC method. Eyes were placed in glass/glass homogenizers containing 1 ml of retinoid analysis buffer (50 mM MOPS, 10 mM NH₂OH, 50% EtOH in H₂O, pH 7.0), and retinoids were extracted with 4 ml of hexane. Extracted retinoids were dried and reconstituted with 300 μ l of hexane prior to loading onto the HPLC silica column.

Retinosome Imaging by Two-photon Microscopy (TPM)—Retinosomes were visualized by TPM using an upright microscope equipped with 20 \times 1.0 NA water immersion objective as described previously (21). RPE cells were cultured in a glass chamber coated with CellStart® (Invitrogen) and incubated at 37 °C until they displayed pigmentation.

Bioluminescence Intensity (BLI) Measurements in Vivo—BLI studies were performed with the Xenogen IVIS 200 system (Caliper Life Sciences) at the Case Western Reserve University Small Animal Imaging Center. Mice were initially administered 125 mg/kg D-luciferin intraperitoneally (Biosynth AG; Staad, Switzerland). The exposure time for each image was 10 min, and images were taken starting 7 min after D-luciferin injection.

Cell Transplantation into the Subretinal Space—All surgical manipulations were carried out under a surgical microscope (Leica M651 MSD). Mice were anesthetized by intraperitoneal injection of 20 μ l/g body weight of 6 mg/ml ketamine and 0.44 mg/ml xylazine diluted with PBS. Pupils were dilated with 1.0% tropicamide. A 33-gauge beveled needle (World Precision Instruments, FL) was used as a lance to make a full-thickness cut through sclera at 1.0 mm posterior to the limbus. The needle was aimed toward the inferior nasal area of the retina and a cell suspension (3×10^4 or 7.5×10^4 cells/eye in 1.5 μ l of Hanks' balanced salt solution) was injected into the subretinal space. Successful administration was confirmed by observing bleb formation. The anti-inflammatory drugs, cyclosporin (210 mg/liter) and minocycline (120 mg/liter) were administered in drinking water starting 1 day before cell transplantation and continuing until experiments were undertaken. The same volume of Hanks' balanced salt solution was injected into the subretinal space as a vehicle control.

Ultra-high Resolution Spectral Domain Optical Coherence Tomography (SD-OCT)—Ultra-high resolution SD-OCT (BiopTigen, NC) was employed for *in vivo* imaging of mouse retinas. Mice were anesthetized by intraperitoneal injection of a mixture (20 μ l/g body weight) containing ketamine (6 mg/ml) and xylazine (0.44 mg/ml) in PBS. Pupils were dilated with 1% tropi-

camide. Four pictures acquired in the B-scan mode were used to construct each final averaged SD-OCT image.

Electroretinograms (ERGs)—All ERG experimental procedures were performed under dim red light transmitted through a Kodak number 1 safelight filter (transmittance >560 nm) as previously noted (20, 22). Briefly, mice first were dark-adapted overnight prior to recording. Then they were anesthetized under a safety light by intraperitoneal injection of 20 μ l/g body weight of 6 mg/ml ketamine and 0.44 mg/ml xylazine diluted with 10 mM sodium phosphate, pH 7.2, containing 100 mM NaCl. Pupils were dilated with 1% tropicamide ophthalmic solution (Bausch and Lomb, Rochester, NY). A contact lens electrode was placed on the eye, and a reference electrode and ground electrode were positioned on the ear and tail, respectively. ERGs were recorded by the universal testing and electrophysiological system (UTAS) with BigShot™ Ganzfeld (LKC Technologies, Gaithersburg, MD). For single-flash recording, white light flash stimuli were employed with a range of intensities (from -3.7 to 1.6 log cd·s·m⁻²), and flash durations were adjusted according to intensity (from 20 μ s to 1 ms). Two to five recordings were made at sufficient intervals between flash stimuli (from 3 s to 1 min) to allow mice time to recover.

Histology—Histological and immunohistochemical procedures used were well established in our laboratory (20). Eye cups for histology were fixed in 2% glutaraldehyde/4% paraformaldehyde and processed for embedding in Epon. Sections were cut at 1 μ m and stained with toluidine blue. Electron microscopy analyses were performed as described previously (20). Anti-LRAT mouse monoclonal antibody and anti-RPE65 mouse monoclonal antibody also were prepared as described (14, 19). Anti-rhodopsin mouse monoclonal antibody (1D4) was a generous gift from Dr. R. S. Molday (University of British Columbia, Vancouver, CA).

Statistical Analyses—Data representing the means \pm S.D. for the results of at least three independent experiments were compared by one-way analysis of variance.

RESULTS

Human iPS Cells Differentiate into RPE Cells—To test whether transplantation of RPE cells with a functional visual cycle can rescue visual function and restore retinal architecture in retinal diseases, RPE cells were induced to differentiate from two different lines of hiPS cells (line 1, HiPS-RIKEN-1A; and line 2, CWRU22) following the protocol used in a previous publication (17). hiPS-RPE cells from both lines showed pigmentation and morphology similar to mpRPE cells from WT mice at passage 3 (P3) (Fig. 1A, upper). Expression of RPE-specific protein, RPE65, also was detected in both hiPS-RPE and mpRPE cells (Fig. 1A, lower). Expression of several visual cycle proteins present in the RPE, namely, RPE65, RDH5, STRA6, CRALBP (RLBP1), and LRAT (10, 11), was examined by RT-PCR in hiPS-RPE cell lines derived from two independent hiPS cell lines from different donors. Two hiPS-RPE cell lines revealed similar amplified bands (Fig. 1B). RPE65 expression was also examined by immunoblots of lysates from mpRPE and hiPS-RPE cells (Fig. 1C). mpRPE and hiRPE expressed RPE65, but RPE65 expression was not detected in immortalized human RPE, ARPE19 cells, similar to the results of RT-PCR in Fig. 1B.

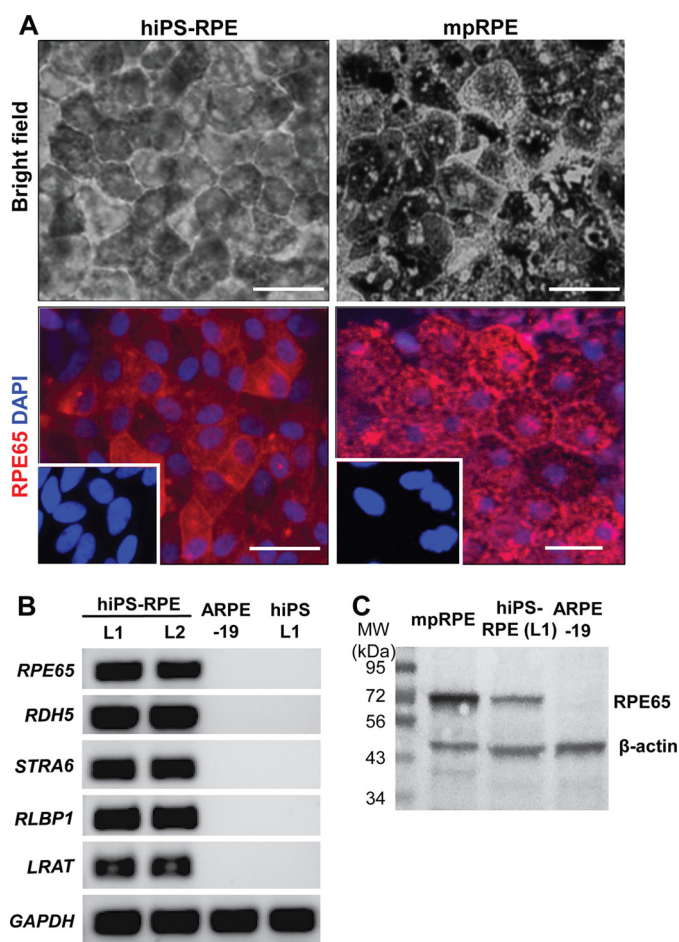


FIGURE 1. Characterization of RPE cells and their expression of visual cycle-associated proteins. *A*, bright field images of hiPS-RPE differentiated from HiPS-RIKEN-1A and WT mpRPE cells are shown (*upper panels*). Immunocytochemistry of hiPS-RPE and mpRPE cells was carried out with anti-RPE65 Ab. Expression of RPE65 (*red*) was detected in both types of cells. Nuclei were stained with DAPI. *Insets* reveal only secondary Ab and DAPI staining. *Scale bars*, 40 μ m. *B*, expression of RPE proteins involved in the visual cycle was examined by RT-PCR in two different lines of hiPS-RPE cells (L1, HiPS-RIKEN-1A; and L2, CWRU22) after the second passage, and in both control ARPE-19 and hiPS cells (L1, HiPS-RIKEN-1A). *C*, immunoblotting was done with anti-RPE65 Ab immediately after isolating mpRPE cells and after the second passage of hiPS-RPE (L1: HiPS-RIKEN-1A) and ARPE19 cells. Cell lysates were prepared by Nonidet P-40 lysis buffer.

hiPS-RPE Cells Maintain Expression of Visual Cycle Proteins—These data indicate that hiPS cells successfully differentiated into RPE cells capable of expressing visual cycle proteins. Previous studies reported decreased expression of visual cycle proteins either during cell culture (23) or under conditions of stress (24). To examine expression of these proteins under our cell culture conditions, we performed qRT-PCR on cells at two different time points with both hiPS-RPE (line 1) and mpRPE cells. In hiPS-RPE cells, visual cycle proteins displayed similar expression levels at passage 4 (P4) and cells at P6 derived from P4 cells 8 weeks later (Fig. 2*A*, *left*). (P2–P4 hiPS-RPE cells were used for *in vitro* testing for 11-*cis*-retinal regeneration in Fig. 3 and transplantation in Fig. 6.) In contrast, markedly decreased expression of these proteins was exhibited by mpRPE cells after 4 weeks in culture (Fig. 2*A*, *right*). Among these proteins, RPE65 expression showed the largest decrease, demonstrating <0.1% of its initial expression determined immediately after harvest-

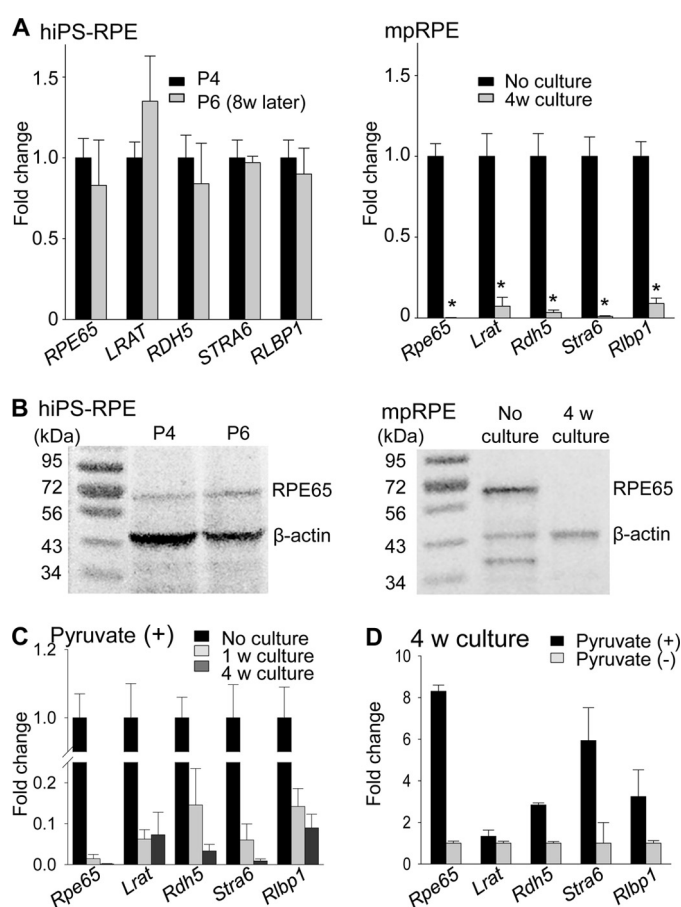


FIGURE 2. Expression levels of RPE65 in hiPS-RPE and mpRPE cells. *A*, expression of visual cycle-associated proteins was examined by qRT-PCR in hiPS-RPE cells at passage 4 (P4) and passage 6 (P6) (*left*). Harvesting of P6 cells was performed 8 weeks after P4 cell collection. Quantitative RT-PCR for visual cycle proteins was also performed with mpRPE cells immediately after their isolation from C57BL/6J mice and 4 weeks after culture (*right*). Relative expression levels against P4 in hiPS-RPE cells and no culture in mpRPE cells are presented. *Error bars* indicate S.D. ($n = 5$). *, $p < 0.001$ versus no culture. Data were normalized against the housekeeping gene, *Gapdh*. *B*, immunoblotting for RPE65 performed with hiPS-RPE cells at P4 and P6 (*left*) and with mpRPE cells immediately after their isolation and after 4 weeks in culture. Cell lysates were prepared by Nonidet P-40 lysis buffer. RPE65 expression was maintained in hiPS-RPE cells, but no RPE65 expression was detected in mpRPE cells after 4 weeks in culture. *C*, effects of pyruvate supplementation. mpRPE cells were isolated from C57BL/6J mice, and expression of visual cycle-associated proteins was examined by qRT-PCR. Data were normalized against the housekeeping gene, *Gapdh*. Expression of visual cycle proteins in mpRPE after 1 and 4 weeks of culture was compared with that of cells placed in medium with 1 mM pyruvate immediately after isolation. Relative expression levels against no cultured mpRPE cells are presented. *Error bars* indicate S.D. ($n = 3 - 5$). *D*, expression of visual cycle proteins in mpRPE cells after 4 weeks of culture in medium with or without 1 mM pyruvate. Relative expression levels against cultured mpRPE cells without pyruvate are presented. *Error bars* indicate S.D. ($n = 3 - 5$).

ing. Immunoblots also revealed RPE65 expression in hiPS-RPE but not mpRPE cells after culture (Fig. 2*B*). We also evaluated expression levels of visual cycle-related genes in mpRPE in the presence of pyruvate in the cell culture medium because pyruvate supplementation can facilitate RPE65 expression in ARPE19 cells (25). Pyruvate supplementation did not maintain the expression of visual cycle protein genes in mpRPE cells (Fig. 2*C*), even though it supported an 8-fold higher expression level of *Rpe65* compared with cells cultured without pyruvate (Fig. 2*D*).

Transplantation of Functional RPE Rescues Vision in Mice

A hiPS-RPE+*Lrat*^{-/-}retina+CRALBP

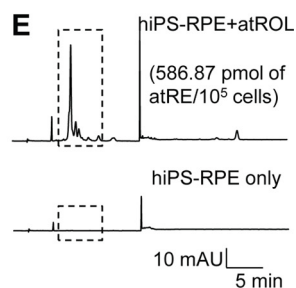
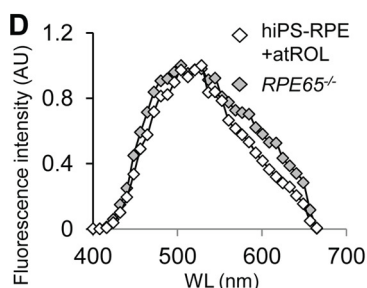
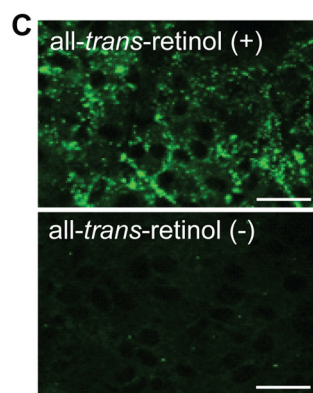
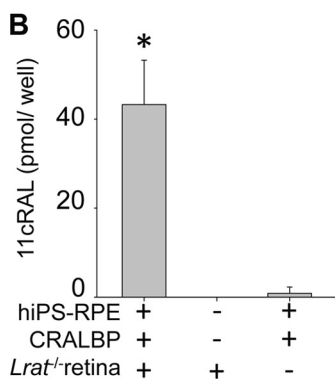
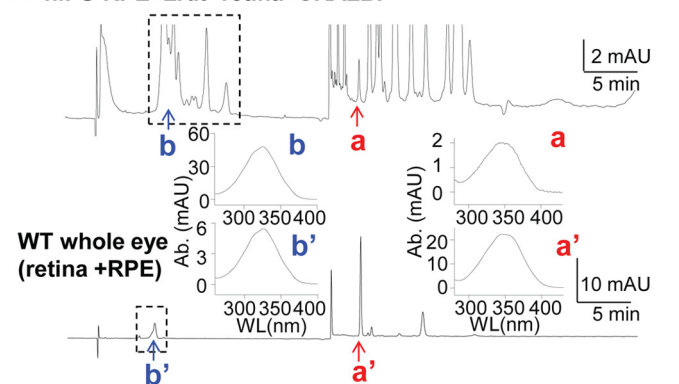


FIGURE 3. Human iPS-RPE cells regenerate visual chromophore. *A*, hiPS-RPE cells at 3×10^4 cells/well (P2–P4 stage) were seeded into 48-well plates, and one retina obtained from a 3-week-old *Lrat*^{-/-} mouse was placed into each well to attach the photoreceptor side to RPE cells in the presence of $30 \mu\text{M}$ recombinant CRALBP. To initiate isomerization, $10 \mu\text{M}$ all-*trans*-retinol was mixed into the cell culture medium, and the plates were incubated at 37°C for 16 h in the dark. Retinoid analyses were performed on retinas after the incubation. A representative chromatogram of retinoids in a WT eye is presented in the lower panel. Red arrows *a* and *a'* indicate 11-*cis*-retinal (syn) peaks. Each inset of the chromatogram shows the spectrum of each peak. Peaks inside the broken line boxes in the chromatograms indicate retinyl esters. Blue arrows *b* and *b'* indicate all-*trans*-retinyl esters. The spectrum of each *b* or *b'* peak is shown as an inset. mAU, milli-absorbance units. *B*, 11-*cis*-retinal produced by hiPS-RPE cells after incubation in the presence of CRALBP and/or *Lrat*^{-/-} retina was quantified by HPLC as described above ($n = 3$ per group). *C*, formation of retinosomes was examined by TPM. hiPS-RPE cells at 3×10^4 cells/well were seeded onto glass bottom culture dishes and cultured for 4 weeks until they became pigmented. Cells were incubated in the presence of $10 \mu\text{M}$ all-*trans*-retinol for 24 h before imaging. Retinosomes appeared as green punctate signals close to cell-cell junctions after incubation with all-*trans*-retinol, whereas these signals were absent in cells without all-*trans*-retinol. *D*, fluorescence spectra of retinosomes from both hiPS-RPE cells after incubation with $10 \mu\text{M}$ all-*trans*-retinol and from eyes of *Rpe65*^{-/-} mice are presented. *Rpe65*^{-/-} mice accumulate retinyl esters in their retinosomes (15, 27). *E*, retinoid content was determined by HPLC after TPM analyses. After hiPS-RPE cells were incubated with $10 \mu\text{M}$ all-*trans*-retinol for 24 h, production of retinyl esters was detected (upper panels). Peaks inside the broken line boxes correspond to peaks of retinyl esters. atRE, all-*trans*-retinyl esters; atROL, all-*trans*-retinol; WL, wavelength. *, $p < 0.05$. Error bars in *B* indicate S.D. ($n = 3$). Scale bars in *C* indicate $20 \mu\text{m}$.

hiPS-RPE Cells Regenerate Visual Chromophore—Because expression of visual cycle proteins was confirmed in hiPS-RPE cells (Figs. 1 and 2), these cells were tested for regeneration of the visual chromophore, 11-*cis*-retinal. hiPS-RPE cells at P2–P4 stage were seeded onto 48-well plates at 3×10^4 cells/well, and a neural retina obtained from one eye of a *Lrat*^{-/-} mouse was placed to attach the photoreceptor outer segment side to these hiPS-RPE cells in each well in the presence of $30 \mu\text{M}$ recombinant CRALBP. The *Lrat*^{-/-} neural retina was used as the source of empty apoprotein, opsin, wherein 11-*cis*-retinal from hiPS-RPE cells can bind to opsin and be stored in the outer segments because 11-*cis*-retinal exists at only at trace levels in *Lrat*^{-/-} eye (14). To initiate isomerization, $10 \mu\text{M}$ all-*trans*-retinol was added to each well, and the plates were incubated at 37°C for 16 h in the dark. Then retinoids in each sample were analyzed by HPLC, and production of 11-*cis*-retinal was detected by the appearance of its spectrum in these samples (Fig. 3A). Formation of retinyl esters also was evident as indicated in the HPLC signals (broken line boxes in Fig. 3A). hiPS-RPE cells (line 1) produced 11-*cis*-retinal (Fig. 3B), suggesting the presence of a functional visual cycle in these cells. Moreover, production of 11-*cis*-retinal also required the presence of CRALBP, a binding partner of 11-*cis*-retinal in the RPE; addition of CRALBP alone to hiPS-RPE cells also produced detectable amounts of 11-*cis*-retinal (Fig. 3B). Because retinyl esters are stored in RPE cell retinosomes when all-*trans*-retinol is successfully esterified by LRAT (26), we then examined the formation of retinosomes by TPM. Retinosome formation was observed after hiPS-RPE cells were co-incubated with $10 \mu\text{M}$ all-*trans*-retinol at 37°C for 16 h, whereas no retinosomes were seen without all-*trans*-retinol (Fig. 3C). Further fluorescence spectra of retinosomes from hiPS-RPE showed a pattern similar to that observed in *Rpe65*^{-/-} mice which display accumulation of retinyl esters in retinosomes (15, 27) (Fig. 3D). Quantification by HPLC revealed 586.9 pmol of all-*trans*-retinyl esters (dotted line rectangle in Fig. 3E) produced from 1×10^5 hiPS-RPE cells after incubation with $10 \mu\text{M}$ all-*trans*-retinol, but no production was detected in the absence of all-*trans*-retinol. Together these data indicate that hiPS-RPE cells possess a functional visual cycle essential for 11-*cis*-retinal regeneration.

Transplantation of Mouse Primary RPE from WT Mice Recovers Visual Function in Retinal Degeneration Mouse Models—It was reported that allogenic transplantation of mpRPE into mouse subretinal space was feasible because transplanted mpRPE cells seemed to be integrated into the host RPE layer morphologically and functionally (28). Based on this intriguing result, we evaluated the viability of transplanted mpRPE cells in host eyes. To address this point, we isolated mpRPE cells from luciferase transgene mice, FVB-Tg (CAG-Luc, GFP) mice, which had been back-crossed with C57BL/6J mice and systematically expressed luciferase under a CAG promoter. We confirmed luciferase activity with cell lysate of mpRPE (Luc-mpRPE) from this strain (data not shown) with a conventional luciferase assay. We then transplanted Luc-mpRPE cells into the subretinal space of albino C57BL/6J-*Tyr*^{*c-2J*}/J mice that allowed recognition of transplanted RPE cells with pigmentation. There were two reasons for using the cited combination of mouse strains for this experiment. First

Transplantation of Functional RPE Rescues Vision in Mice

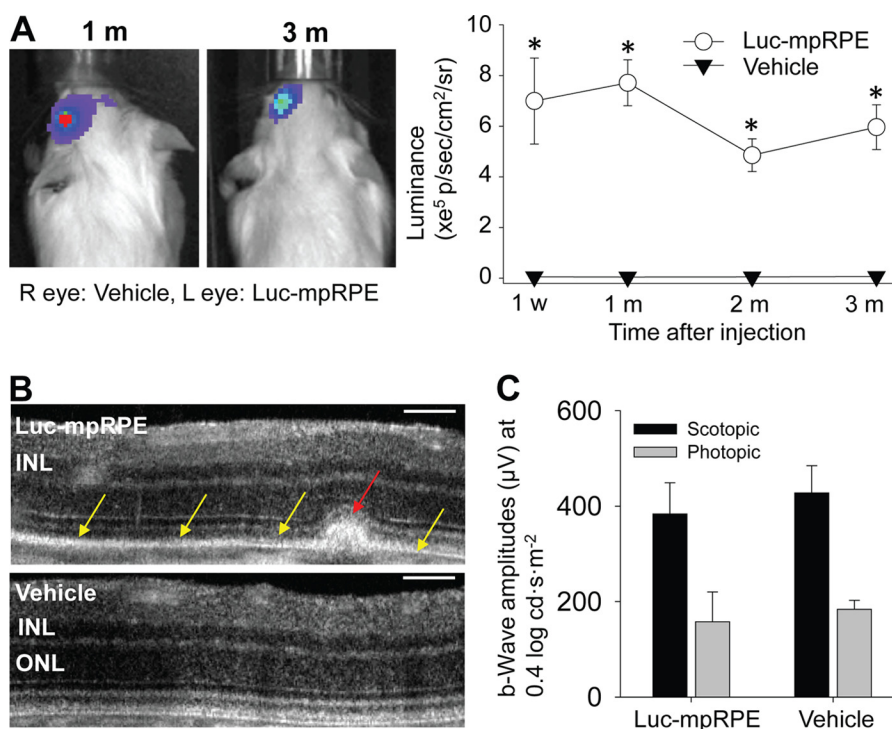


FIGURE 4. Transplantation of mouse primary RPE cells into the subretinal space of WT mice. *A*, mpRPE cells isolated from luciferase-transgenic mice (Luc-mpRPE) were transplanted into the subretinal space of 6–8-week-old albino C57BL/6J mice at 3×10^4 cells/eye. BLI assay of mouse eyes displayed a positive intensity in eyes at 1 and 3 min after transplantation, but a BLI signal was not detected in eyes treated with vehicle only (*left panel*). The intensity of BLI was measured 1 week and 1, 2, and 3 months after transplantation (*right panel*). Error bars indicate S.E. ($n = 5$). *B*, SD-OCT images show a retinal cross-section at a Luc-mpRPE transplanted lesion (*upper panel*). Even though aggregate-like structures were noted sporadically in the subretinal space (*red arrow*), there were no other obvious disruptions in the RPE layer (*yellow arrows*) and retinal morphology of the transplant. SD-OCT images from vehicle-treated eyes showed normal morphology of the retina (*lower panel*). INL, inner nuclear layer; ONL, outer nuclear layer. *C*, ERG recordings at $0.4 \log \text{cd} \cdot \text{s} \cdot \text{m}^{-2}$ under scotopic and photopic conditions. Functional b-wave amplitudes obtained from eyes with Luc-mpRPE or vehicle treatment were plotted. Error bars indicate S.D. ($n = 3$).

was the expectation of a minimal graft *versus* host reaction with this combination of strains. Second, no protocol to differentiate RPE cells from mouse iPS cells was currently available. In addition, we treated the transplanted mice with two systemically administered immunosuppressants, minocycline and cyclosporin A. Survival of transplanted cells was examined with the BLI assay carried out at 1 week, 1 month, 2 months, and 3 months after Luc-mpRPE transplantation. Eyes transplanted with Luc-mpRPE displayed increased luminance (Fig. 4A, *left*). Although this intensity decreased with time, relatively strong signals were still detected 3 months after transplantation when cyclosporin (for T cell inactivation) and minocycline (for anti-microglial effects) (29) were administered (Fig. 4A, *right*). We also evaluated the effects of Luc-mpRPE transplantation on the morphology and function of the retina. SD-OCT images 3 months after transplantation revealed aggregate-like structures of various sizes sporadically distributed in the subretinal space (*red arrow*, Fig. 4B); otherwise the photoreceptor (ONL) and RPE layers (*yellow arrows*, Fig. 4B) were relatively well maintained. Single flash ERG recordings showed that both scotopic and photopic responses were mildly but not significantly attenuated ($p > 0.45$) 3 months after transplantation (Fig. 4C), findings consistent with a previous study (28). These data indicate that transplanted RPE cells can survive for months under anti-inflammatory conditions.

Having shown that transplanted mpRPE cells can survive *in vivo*, we transplanted 3×10^4 mpRPE cells from C57BL/6J mice into the subretinal space of albino *Lrat*^{-/-} mice and *Rpe65*^{-/-}

mice, mouse models of LCA. *Lrat*^{-/-} mice cannot produce endogenous 11-*cis*-retinal, and all-*trans*-retinyl esters also fail to display functional ERG responses (14). We performed transscleral TPM aimed at transplanted mpRPE cell layer (*red arrow* in Fig. 5A) to evaluate all-*trans*-retinyl ester formation *ex vivo*. Clusters of fluorescence signals from retinosomes were detected in TPM images of transplanted mpRPE in TPM images (Fig. 5, *B* and *C*). The spectra of signals obtained from these retinosomes were similar (Fig. 5D) to those obtained from *Rpe65*^{-/-} mice (Fig. 3D). Survival of transplanted mpRPE cells was further documented by observance of pigmented RPE cells in retinal cross-sections (Fig. 5Ea). Transmission electron microscope (TEM) images of these pigmented mpRPE cells showed phagosomes (*red arrow* in Fig. 5Eb) and melanosomes in the cytoplasmic space of mpRPE cells, whereas melanosomes were not observed in host RPE cells without pigmentation adjacent to the transplant (Fig. 5Ec). These data show that surviving transplanted mpRPE cells can exhibit key cellular functions of RPE cells in the subretinal space. Retinoid analyses of these mpRPE cell-transplanted eyes demonstrated endogenous production of 11-*cis*-retinal and all-*trans*-retinyl esters 1 and 3 months after mpRPE transplantation (Fig. 5F). Improved retinal function was also documented by scotopic ERG recordings 1 and 3 months after mpRPE transplantation (Fig. 5G). We also tested efficacy of transplanting mpRPE cells from C57BL/6J mice into in *Rpe65*^{-/-} mice. Functional recovery of the visual cycle in albino *Rpe65*^{-/-} mice was evidenced by detection of 11-*cis*-retinal by HPLC 3 months after transplantation (Fig. 5H)

Transplantation of Functional RPE Rescues Vision in Mice

WT mpRPE transplantation into *Lrat*^{-/-} mice

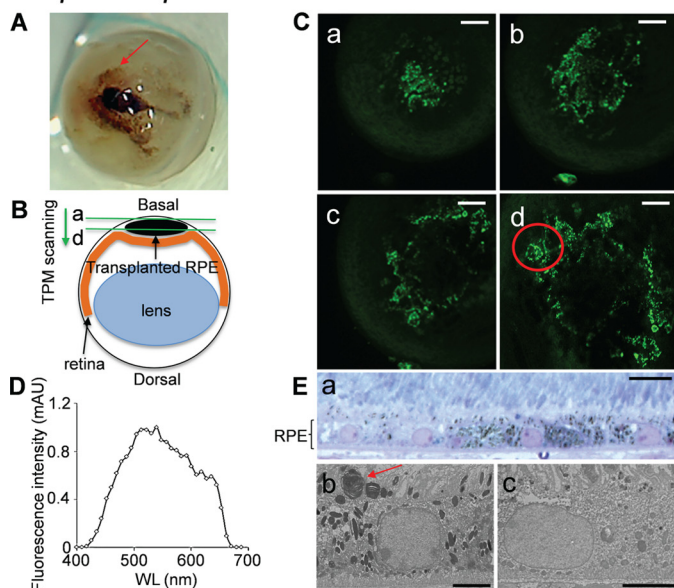
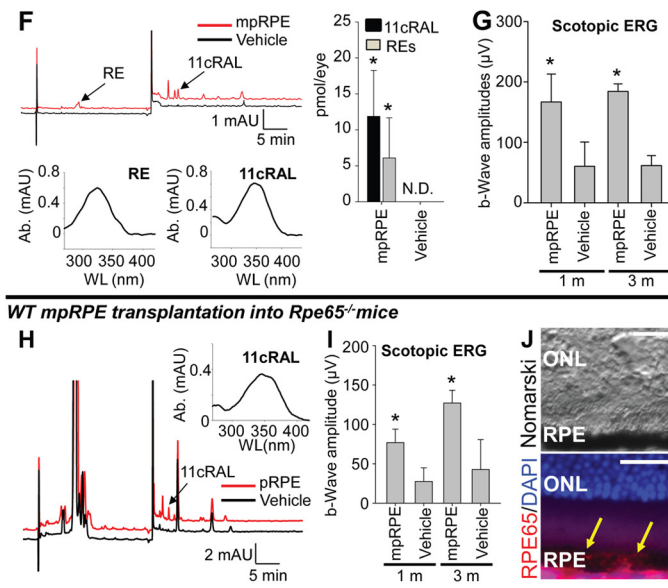


FIGURE 5. Transplantation of mouse primary RPE cells into subretinal space of genetically altered mouse models. A–G, mpRPE cells were isolated from C57BL/6J mice, and 3×10^4 cells in $1.5 \mu\text{l}/\text{eye}$ were transplanted into the subretinal space of 3-week-old albino *Lrat*^{-/-} mice with a C57BL/6J background. A, representative image shows transplanted eye. TPM images were obtained from the transplant (red arrow) through the sclera at the basal side of the eye. B, the transplant was scanned by TPM from a surface plane (a) to a deeper plane (d). C, fluorescence signals from retinosomes were observed in TPM images obtained from each plane (a–d). Scale bars indicate $20 \mu\text{m}$. D, fluorescence spectrum of the red-circled lesion in d of C is presented. The pattern of spectrum is comparable with that from WT and *Rpe65*^{-/-} mice as shown in Fig. 3D. mAU, milli-absorbance units; WL, wavelength. E, representative retinal cross-section images of mpRPE transplants were prepared 3 months after transplantation. Transplanted mpRPE cells with pigmentation were observed in the subretinal space as a monolayer (a) adjacent to the host RPE cells without pigmentation. Detailed morphology of the transplanted mpRPE cells was imaged further by TEM (b), which revealed melanosomes that were absent in host RPE cells (c). The phagocytosed rod outer segment indicated with a red arrow shows that transplanted RPE cells have the ability to carry out phagocytosis. Scale bars in both a and b indicate $5 \mu\text{m}$; that in c indicates $2 \mu\text{m}$. F, retinoid analyses performed 3 months after transplantation show that production of retinyl esters (RE) and 11-cis-retinal (11cRAL) was detected only in mpRPE-cell transplanted eyes. Spectra of RE and 11cRAL are presented in the bottom row, and quantified amounts are shown in the right panel. Error bars indicate S.D. ($n = 5$). *, $p < 0.05$. G, ERGs recorded at 1 and 3 months after mpRPE transplantation show restoration of retinal function in mpRPE cell transplanted *Lrat*^{-/-} eyes. N.D., not detectable. H–J, mpRPE cells were transplanted into the subretinal space of 3-week-old albino *Rpe65*^{-/-} mice with a C57BL/6J background at 3.0×10^4 cells/eye. H, in retinoid analyses performed 3 months after transplantation, 11-cis-retinal (11cRAL) was detected in *Rpe65*^{-/-} eyes treated with mpRPE cells. Absorbance spectra of 11cRAL indicated an 11-cis-retinal specific pattern. WL, wavelength. I, ERGs recorded 1 and 3 months after the transplantation indicate preservation of scotopic visual function in mpRPE cell transplants. J, RPE65 expression was confirmed by immunohistochemistry in mpRPE cell transplanted *Rpe65*^{-/-} retina (yellow arrows). ONL, outer nuclear layer. Error bars in I indicate S.D. Scale bars in J indicate $20 \mu\text{m}$. *, $p < 0.05$. For *Rpe65*^{-/-} mice study, $n = 3$ –5/group for ERGs; $n = 2$ for retinoid analyses.

and improvement of b-wave amplitudes of scotopic ERGs 1 and 3 months after transplantation (Fig. 5I). Survival of transplanted mpRPE cells was further documented by immunohistochemistry of retinal cross-sections with anti-RPE65 antibody that revealed expression of RPE65 in pigmented RPE cells 3 months after transplantation (Fig. 5J).

hiPS-RPE Cells Are Functional When Transplanted into Mouse Models of Retinal Degeneration—Finally, we investigated the functionality of the visual cycle in hiPS-RPE cells *in vivo*. P2–P4 stages of hiPS-RPE cells at 7.5×10^4 cells/eye were transplanted into both 3-week-old albino *Lrat*^{-/-} mice and *Rpe65*^{-/-} mice. Improvement of b-wave amplitudes of scotopic ERGs were observed in albino *Lrat*^{-/-} mice 1 and 3 months after transplantation (Fig. 6A). Moreover, successful transplantation and morphological maintenance of the outer nuclear layer in the retina were confirmed at the injected site as shown by an SD-OCT image obtained 1 month after transplantation (Fig. 6B, upper panel). Pigmented RPE cells were observed locally in the host RPE cell layer 3 months after transplantation (Fig. 6B, lower panel). LRAT expression in transplanted hiPS-RPE cells and the interface between RPE cells and rod outer segments was evaluated by immunohistochemistry with anti-LRAT and anti-rhodopsin antibodies. Cells with pig-



WT mpRPE transplantation into *Rpe65*^{-/-} mice

H, in retinoid analyses performed 3 months after transplantation, 11-cis-retinal (11cRAL) was detected in *Rpe65*^{-/-} eyes treated with mpRPE cells. Absorbance spectra of 11cRAL indicated an 11-cis-retinal specific pattern. WL, wavelength. I, ERGs recorded 1 and 3 months after the transplantation indicate preservation of scotopic visual function in mpRPE cell transplants. J, RPE65 expression was confirmed by immunohistochemistry in mpRPE cell transplanted *Rpe65*^{-/-} retina (yellow arrows). ONL, outer nuclear layer. Error bars in I indicate S.D. Scale bars in J indicate $20 \mu\text{m}$. *, $p < 0.05$. For *Rpe65*^{-/-} mice study, $n = 3$ –5/group for ERGs; $n = 2$ for retinoid analyses.

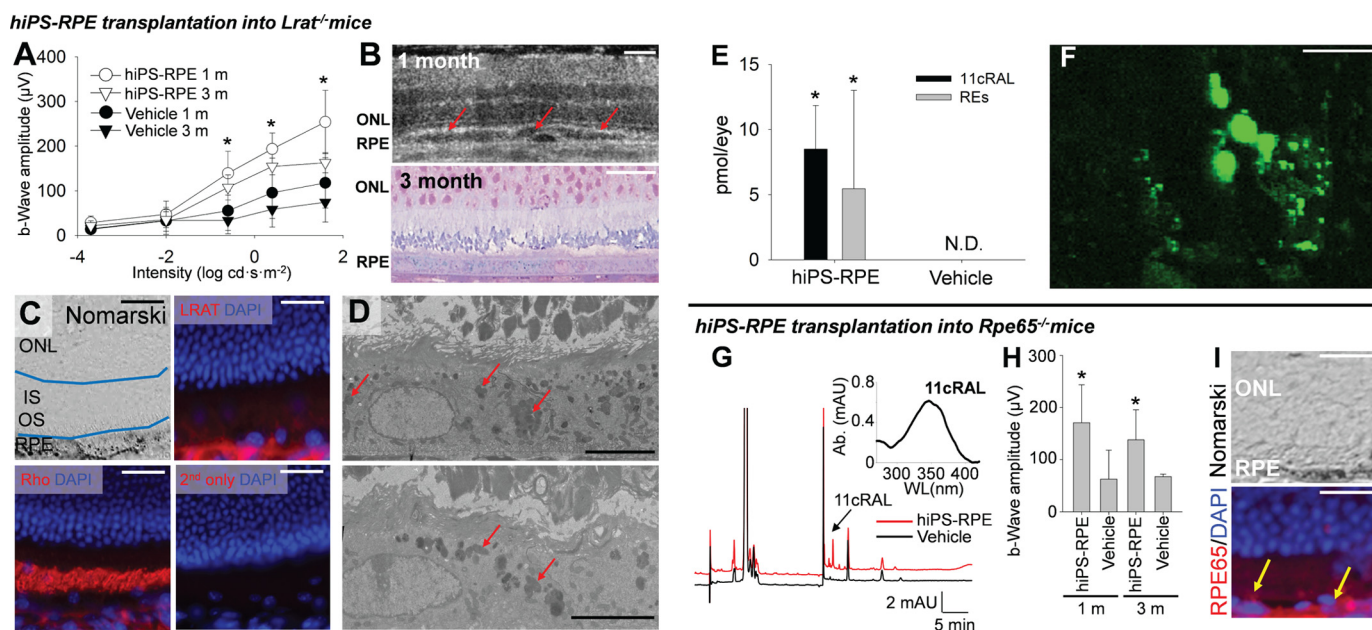


FIGURE 6. Transplantation of hiPS-RPE cells into the subretinal space of genetically altered mouse models. hiPS-RPE cells (P2–P4 stage), 7.5×10^4 cells/eye, were transplanted into the subretinal space of 3-week-old albino *Lrat*^{-/-} mice with a C57BL/6J background. These mice were treated with cyclosporin and minocycline in their drinking water over the 3-month experimental period. **A**, ERGs were recorded at 1 and 3 months after transplantation. *, $p < 0.05$; $n = 3–5$. **B**, the transplanted cells were seen after SD-OCT examination 1 month after transplantation (red arrows in upper panel) and also found as a monolayer of cells with pigmentation in albino *Lrat*^{-/-} mice 3 months after transplantation (lower panel). ONL, outer nuclear layer. Scale bars in upper and lower panels indicate 40 and 10 μm , respectively. **C**, immunohistochemical images show transplants in *Lrat*^{-/-} mice at 3 months after transplantation after staining with anti-LRAT antibody, rhodopsin (*Rho*) antibody and DAPI for nuclei. Scale bars indicate 20 μm . IS, inner segment; OS, outer segment. **D**, detailed morphology of transplanted hiPS-RPE cells was examined by TEM imaging. Two images captured from the different areas of the transplanted region are shown. Melanosomes and villus formation were observed in the cytoplasmic space and dorsal region of RPE cells (red arrows). Scale bars indicate 4 μm . **E**, retinoid analyses were performed by HPLC 3 months after transplantation. Error bars indicate S.D. ($n = 3$). **F**, fluorescence signals from retinosomes of transplanted hiPS-RPE cells were detected by TPM. **G–I**, hiPS-RPE cells were transplanted into the subretinal space of 3-week-old albino *Rpe65*^{-/-} mice with a C57BL/6J background at 7.5×10^4 cells/eye. **G**, retinoid analyses performed by HPLC 3 months after transplantation show that 11-*cis*-retinal (11cRAL) was detected in *Rpe65*^{-/-} eyes treated with hiPS-RPE cells. Absorbance spectra of 11cRAL indicated an 11-*cis*-retinal specific pattern (inset). WL, wavelength. **H**, ERGs recorded 1 and 3 months after the transplantation indicated preservation of hiPS-RPE function. **I**, RPE65 expression was confirmed by immunohistochemistry in hiPS-RPE transplanted *Rpe65*^{-/-} retina (yellow arrows). Error bars in **H** indicate S.D. Scale bars in **I** indicate 20 μm . *, $p < 0.05$. For the *Rpe65*^{-/-} mouse studies, $n = 3–5$ /group for ERGs and $n = 2$ for retinoid analyses.

of RPE65 in pigmented RPE cells 3 months after transplantation (Fig. 6I).

DISCUSSION

Clinical use of cells differentiated from iPS cells is gaining popularity because iPS cells allow the production of any type of cell without destruction of embryonic cells, thus avoiding complex ethical issues and providing a unique therapeutic option for currently untreatable diseases such as retinal degeneration. In addition, the use of differentiated cells from iPS cells also provides an opportunity to conduct autologous transplantation with own fibroblast/skin cells from patients. A severe form of congenital retinal degeneration, called Leber congenital amaurosis, is caused by dysfunctional RPE cells. LCA patients exhibit defects in visual cycle enzymes such as LRAT and RPE65. Moreover, other impairments affecting visual cycle components along with defective or absent retinoid-binding proteins also are closely associated with human retinal diseases. Therefore, hiPS-RPE cells with a functional visual cycle could help certain individuals with blinding retinal diseases.

Expression of Visual Cycle Molecules in RPE Cells—Differentiation of RPE cells from ES and iPS cells has been reported (8, 9), and some RPE functions have been characterized in these cells. These include the expression of RPE-specific molecules such as BEST1, MERTK, RPE65, and CRALBP along with the

capability to carry out phagocytosis, form adherence junctions, and produce cytokines (10, 11). Among many important roles of the RPE *in vivo*, one of the most important is to maintain a functional visual cycle essential for vision. Although many human retinal diseases are associated with an abnormal visual cycle, its function has not been well documented in hiPS-RPE cells.

Our study demonstrates that hiPS-RPE cells express important proteins normally found in RPE cells that relate to the visual cycle and that this expression is retained during cell culture (Fig. 2). Although mpRPE cells from WT mice exhibited normal expression immediately after cell isolation, this decreased dramatically during cell culture. Specifically, the decrease in RPE65 was the most prominent, dropping to <1% 1 week after culture and to 0.1% 4 weeks later (Fig. 2C). Because pyruvate supplementation in cell culture medium and postconfluent culture reportedly maintain RPE65 expression levels in ARPE19 cells (25), we compared the expression of visual cycle proteins in mpRPE cells cultured with or without pyruvate. Even though higher expression of these proteins occurred in the presence of pyruvate, the effect was only modest (Fig. 2, C and D). Decreased expression of RPE65 during primary RPE cell culture was previously described when RPE65 was initially characterized in bovine RPE cells (23). Possible explanations

are that aberrant post-translational modifications of RPE65 occurred because of the culture conditions, or unknown transcription factors to the AP-4, nuclear factor one, and octamerous elements could regulate the *Rpe65* promoter activity (30, 31). Other groups reported decreased expression of visual cycle enzymes after light exposure or under conditions of retinal detachment *in vivo* (24, 32). Of note, leukemia inhibitory factor, an interleukin-6 family neurocytokine, could be up-regulated in response to different types of retinal stress and have neuroprotective activity through activation of the gp130 receptor/STAT3 pathway in RPE *in vivo* (32). In primary RPE cells, culture conditions may function as a stress inducer, but induced iPS-RPE cells could already have adjusted to culture conditions. Possibly due to their adaptation to culture conditions, iPS-RPE cells could also maintain their expression of visual cycle proteins. Interestingly, mpRPE cells transplanted into the subretinal space of mice did function (Fig. 5), suggesting that environmental factors are critical for maintaining their visual cycle protein expression. Indeed, it was reported that proper cell contact to extracellular matrix is needed to express important molecules for RPE function, such as RPE65 and ZO-1 (33, 34). Improving culture conditions for iPS-RPE cells has the potential of making them even more suitable for therapeutic applications.

Future Clinical Applications of iPS-RPE Transplantation—Transplantation of RPE cells containing a functional visual cycle partially restored visual function in blind mice (Figs. 5 and 6), indicating that this method could be applicable in rescuing vision in humans who have experienced vision loss due to defects in RPE cells. When examining retinal diseases resulting from an impaired visual cycle, it is apparent that we currently have several potential therapeutic options including gene transfer therapy. RPE65 gene transfer therapy has been initiated for patients with RPE65 mutations, and preliminary results are encouraging (35, 36). Pharmacologic therapy with 9-*cis*-retinoids can restore vision in previously blind mice (37) and dogs (38). When one adds in functional RPE transplantation, it becomes apparent that at least three potential therapies are available for retinal diseases caused by dysfunctional RPE65 and LRAT.

Currently, RPE transplantation is also considered a superior treatment option for patients with AMD, because the primary lesion in this disease occurs in the RPE (39). AMD is a leading cause of legal blindness in industrialized countries. Because the AMD lesion is limited to the central part of the retina, the number of cells required for transplantation is relatively low compared with organ transplants such as liver or heart. Furthermore, transplanted RPE cells can function without having to establish connecting synapses with neurons or other cell types. The existence of a functional visual cycle in hiPS-RPE cells and the restoration of vision in blind mice resulting from the transplantation of hiPS-RPE cells demonstrated in the current study provide additional evidence that should promote the development of hiPS-RPE cells for treatment of retinal diseases. This is reinforced by previous proof of concept studies by other groups using rodent models of retinal dystrophy (6, 40).

Collectively, hiPS-RPE cells were shown here not only to express visual cycle proteins in culture but also to produce

11-*cis*-retinal both *in vitro* and *in vivo*. Given this level of functionality, it is apparent that hiPS-RPE cells could be strong candidates for treatment of retinal degenerative diseases such as retinitis pigmentosa and AMD.

Acknowledgments—We thank Drs. M. Golczak, B. Kevany, J Zhang, L. Cooperman, H. Fujioka, J. Molter, L. Perusek, S. Howell, H. Maeno and S. Donnola (Case Western Reserve University) for comments and technical support and especially Dr. M. Sawada, K. Iseki, and N. Sakai (RIKEN) for technical support.

REFERENCES

1. Jonasson, F., Arnarsson, A., Eiriksdottir, G., Harris, T. B., Launer, L. J., Meuer, S. M., Klein, B. E., Klein, R., Gudnason, V., and Cotch, M. F. (2011) Prevalence of age-related macular degeneration in old persons: Age, Gene/Environment Susceptibility Reykjavik Study. *Ophthalmology* **118**, 825–830
2. Cheung, C. M., Tai, E. S., Kawasaki, R., Tay, W. T., Lee, J. L., Hamzah, H., and Wong, T. Y. (2012) Prevalence of and risk factors for age-related macular degeneration in a multiethnic Asian cohort. *Arch. Ophthalmol.* **130**, 480–486
3. Klein, R., Lee, K. E., Gangnon, R. E., and Klein, B. E. (2013) Incidence of visual impairment over a 20-year period: the Beaver Dam Eye Study. *Ophthalmology* **120**, 1210–1219
4. Coffey, P. J., Girman, S., Wang, S. M., Hetherington, L., Keegan, D. J., Adamson, P., Greenwood, J., and Lund, R. D. (2002) Long-term preservation of cortically dependent visual function in RCS rats by transplantation. *Nat. Neurosci.* **5**, 53–56
5. Tezel, T. H., Del Priore, L. V., Berger, A. S., and Kaplan, H. J. (2007) Adult retinal pigment epithelial transplantation in exudative age-related macular degeneration. *Am. J. Ophthalmol.* **143**, 584–595
6. Carr, A. J., Smart, M. J., Ramsden, C. M., Powner, M. B., da Cruz, L., and Coffey, P. J. (2013) Development of human embryonic stem cell therapies for age-related macular degeneration. *Trends Neurosci.* **36**, 385–395
7. Park, I. H., Arora, N., Huo, H., Maherali, N., Ahfeldt, T., Shimamura, A., Lensch, M. W., Cowan, C., Hochedlinger, K., and Daley, G. Q. (2008) Disease-specific induced pluripotent stem cells. *Cell* **134**, 877–886
8. Carr, A. J., Vugler, A. A., Hikita, S. T., Lawrence, J. M., Gias, C., Chen, L. L., Buchholz, D. E., Ahmado, A., Semo, M., Smart, M. J., Hasan, S., da Cruz, L., Johnson, L. V., Clegg, D. O., and Coffey, P. J. (2009) Protective effects of human iPS-derived retinal pigment epithelium cell transplantation in the retinal dystrophic rat. *PLoS One* **4**, e8152
9. Haruta, M., Sasai, Y., Kawasaki, H., Amemiya, K., Ooto, S., Kitada, M., Suemori, H., Nakatsuji, N., Ide, C., Honda, Y., and Takahashi, M. (2004) *In vitro* and *in vivo* characterization of pigment epithelial cells differentiated from primate embryonic stem cells. *Invest. Ophthalmol. Vis. Sci.* **45**, 1020–1025
10. Tang, P. H., Kono, M., Koutalos, Y., Ablonczy, Z., and Crouch, R. K. (2013) New insights into retinoid metabolism and cycling within the retina. *Prog. Retin. Eye Res.* **32**, 48–63
11. Kiser, P. D., Golczak, M., Maeda, A., and Palczewski, K. (2012) Key enzymes of the retinoid (visual) cycle in vertebrate retina. *Biochim. Biophys. Acta* **1821**, 137–151
12. Marlhens, F., Bareil, C., Griffioen, J. M., Zrenner, E., Amalric, P., Eliaou, C., Liu, S. Y., Harris, E., Redmond, T. M., Arnaud, B., Claustres, M., and Hamel, C. P. (1997) Mutations in *RPE65* cause Leber's congenital amaurosis. *Nat. Genet.* **17**, 139–141
13. Thompson, D. A., Li, Y., McHenry, C. L., Carlson, T. J., Ding, X., Sieving, P. A., Apfelstedt-Sylla, E., and Gal, A. (2001) Mutations in the gene encoding lecithin retinol acyltransferase are associated with early onset severe retinal dystrophy. *Nat. Genet.* **28**, 123–124
14. Batten, M. L., Imanishi, Y., Maeda, T., Tu, D. C., Moise, A. R., Bronson, D., Possin, D., Van Gelder, R. N., Baehr, W., and Palczewski, K. (2004) Lecithin-retinol acyltransferase is essential for accumulation of all-*trans*-retinyl esters in the eye and in the liver. *J. Biol. Chem.* **279**, 10422–10432

15. Redmond, T. M., Yu, S., Lee, E., Bok, D., Hamasaki, D., Chen, N., Goletz, P., Ma, J. X., Crouch, R. K., and Pfeifer, K. (1998) Rpe65 is necessary for production of 11-*cis*-vitamin A in the retinal visual cycle. *Nat. Genet.* **20**, 344–351
16. Diemer, T., Gibbs, D., and Williams, D. S. (2008) Analysis of the rate of disk membrane digestion by cultured RPE cells. *Adv. Exp. Med. Biol.* **613**, 321–326
17. Osakada, F., Ikeda, H., Sasai, Y., and Takahashi, M. (2009) Stepwise differentiation of pluripotent stem cells into retinal cells. *Nat. Protoc.* **4**, 811–824
18. Kanemura, H., Go, M. J., Nishishita, N., Sakai, N., Kamao, H., Sato, Y., Takahashi, M., and Kawamata, S. (2013) Pigment epithelium-derived factor secreted from retinal pigment epithelium facilitates apoptotic cell death of iPSC. *Sci. Rep.* **3**, 2334
19. Golczak, M., Kiser, P. D., Lodowski, D. T., Maeda, A., and Palczewski, K. (2010) Importance of membrane structural integrity for RPE65 retinoid isomerization activity. *J. Biol. Chem.* **285**, 9667–9682
20. Maeda, A., Maeda, T., Imanishi, Y., Kuksa, V., Alekseev, A., Bronson, J. D., Zhang, H., Zhu, L., Sun, W., Saperstein, D. A., Rieke, F., Baehr, W., and Palczewski, K. (2005) Role of photoreceptor-specific retinol dehydrogenase in the retinoid cycle *in vivo*. *J. Biol. Chem.* **280**, 18822–18832
21. Imanishi, Y., Gerke, V., and Palczewski, K. (2004) Retinosomes: new insights into intracellular managing of hydrophobic substances in lipid bodies. *J. Cell Biol.* **166**, 447–453
22. Maeda, T., Lem, J., Palczewski, K., and Haeseleer, F. (2005) A critical role of CaBP4 in the cone synapse. *Invest. Ophthalmol. Vis. Sci.* **46**, 4320–4327
23. Hamel, C. P., Tsilou, E., Pfeffer, B. A., Hooks, J. J., Detrick, B., and Redmond, T. M. (1993) Molecular cloning and expression of RPE65, a novel retinal pigment epithelium-specific microsomal protein that is post-transcriptionally regulated *in vitro*. *J. Biol. Chem.* **268**, 15751–15757
24. Rattner, A., Toulabi, L., Williams, J., Yu, H., and Nathans, J. (2008) The genomic response of the retinal pigment epithelium to light damage and retinal detachment. *J. Neurosci.* **28**, 9880–9889
25. Ahmado, A., Carr, A. J., Vugler, A. A., Semo, M., Gias, C., Lawrence, J. M., Chen, L. L., Chen, F. K., Turowski, P., da Cruz, L., and Coffey, P. J. (2011) Induction of differentiation by pyruvate and DMEM in the human retinal pigment epithelium cell line ARPE-19. *Invest. Ophthalmol. Vis. Sci.* **52**, 7148–7159
26. Imanishi, Y., Batten, M. L., Piston, D. W., Baehr, W., and Palczewski, K. (2004) Noninvasive two-photon imaging reveals retinyl ester storage structures in the eye. *J. Cell Biol.* **164**, 373–383
27. Palczewska, G., Maeda, T., Imanishi, Y., Sun, W., Chen, Y., Williams, D. R., Piston, D. W., Maeda, A., and Palczewski, K. (2010) Noninvasive multiphoton fluorescence microscopy resolves retinol and retinal condensation products in mouse eyes. *Nat. Med.* **16**, 1444–1449
28. Engelhardt, M., Tosha, C., Lopes, V. S., Chen, B., Nguyen, L., Nusinowitz, S., and Williams, D. S. (2012) Functional and morphological analysis of the subretinal injection of retinal pigment epithelium cells. *Vis. Neurosci.* **29**, 83–93
29. Yrjänheikki, J., Keinänen, R., Pellikka, M., Hökfelt, T., and Koistinaho, J. (1998) Tetracyclines inhibit microglial activation and are neuroprotective in global brain ischemia. *Proc. Natl. Acad. Sci. U.S.A.* **95**, 15769–15774
30. Boulanger, A., Liu, S., Henningsgaard, A. A., Yu, S., and Redmond, T. M. (2000) The upstream region of the *Rpe65* gene confers retinal pigment epithelium-specific expression *in vivo* and *in vitro* and contains critical octamer and E-box binding sites. *J. Biol. Chem.* **275**, 31274–31282
31. Nicoletti, A., Kawase, K., and Thompson, D. A. (1998) Promoter analysis of *RPE65*, the gene encoding a 61-kDa retinal pigment epithelium-specific protein. *Invest. Ophthalmol. Vis. Sci.* **39**, 637–644
32. Chucair-Elliott, A. J., Elliott, M. H., Wang, J., Moiseyev, G. P., Ma, J. X., Politi, L. E., Rotstein, N. P., Akira, S., Uematsu, S., and Ash, J. D. (2012) Leukemia inhibitory factor coordinates the down-regulation of the visual cycle in the retina and retinal-pigmented epithelium. *J. Biol. Chem.* **287**, 24092–24102
33. Stanzel, B. V., Espana, E. M., Grueterich, M., Kawakita, T., Parel, J. M., Tseng, S. C., and Binder, S. (2005) Amniotic membrane maintains the phenotype of rabbit retinal pigment epithelial cells in culture. *Exp. Eye Res.* **80**, 103–112
34. Chen, H. C., Zhu, Y. T., Chen, S. Y., and Tseng, S. C. (2012) Wnt signaling induces epithelial-mesenchymal transition with proliferation in ARPE-19 cells upon loss of contact inhibition. *Lab. Invest.* **92**, 676–687
35. Maguire, A. M., Simonelli, F., Pierce, E. A., Pugh, E. N., Jr., Mingozzi, F., Bencicelli, J., Banfi, S., Marshall, K. A., Testa, F., Surace, E. M., Rossi, S., Lyubarsky, A., Arruda, V. R., Konkle, B., Stone, E., Sun, J., Jacobs, J., Dell’Osso, L., Hertle, R., Ma, J. X., Redmond, T. M., Zhu, X., Hauck, B., Zelenia, O., Shindler, K. S., Maguire, M. G., Wright, J. F., Volpe, N. J., McDonnell, J. W., Auricchio, A., High, K. A., and Bennett, J. (2008) Safety and efficacy of gene transfer for Leber’s congenital amaurosis. *N. Engl. J. Med.* **358**, 2240–2248
36. Bainbridge, J. W., Smith, A. J., Barker, S. S., Robbie, S., Henderson, R., Balaggan, K., Viswanathan, A., Holder, G. E., Stockman, A., Tyler, N., Petersen-Jones, S., Bhattacharya, S. S., Thrasher, A. J., Fitzke, F. W., Carter, B. J., Rubin, G. S., Moore, A. T., and Ali, R. R. (2008) Effect of gene therapy on visual function in Leber’s congenital amaurosis. *N. Engl. J. Med.* **358**, 2231–2239
37. Van Hooser, J. P., Aleman, T. S., He, Y. G., Cideciyan, A. V., Kuksa, V., Pittler, S. J., Stone, E. M., Jacobson, S. G., and Palczewski, K. (2000) Rapid restoration of visual pigment and function with oral retinoid in a mouse model of childhood blindness. *Proc. Natl. Acad. Sci. U.S.A.* **97**, 8623–8628
38. Gearhart, P. M., Gearhart, C., Thompson, D. A., and Petersen-Jones, S. M. (2010) Improvement of visual performance with intravitreal administration of 9-*cis*-retinal in *Rpe65*-mutant dogs. *Arch. Ophthalmol.* **128**, 1442–1448
39. Schwartz, S. D., Hubschman, J. P., Heilwell, G., Franco-Cardenas, V., Pan, C. K., Ostrick, R. M., Mickunas, E., Gay, R., Klimanskaya, I., and Lanza, R. (2012) Embryonic stem cell trials for macular degeneration: a preliminary report. *Lancet* **379**, 713–720
40. Lu, B., Malcuit, C., Wang, S., Girman, S., Francis, P., Lemieux, L., Lanza, R., and Lund, R. (2009) Long-term safety and function of RPE from human embryonic stem cells in preclinical models of macular degeneration. *Stem Cells* **27**, 2126–2135